A Two Dimensional Inverse Scattering Problem for Shape and Conductive Function for a Dielectic Cylinder

Ahmet Altundag

Abstract The inverse problem under consideration is to simultaneously reconstruct the conductive function and shape of a coated homogeneous dielectric infinite cylinder from the far-field pattern for scattering of a time-harmonic E-polarized electromagnetic plane wave. We propose an inverse algorithm that combine the approaches suggested by Ivanyshyn et al. [1–3], and extend the approaches from the case of impenetrable scatterer to the case of penetrable scatterer. It is based on a system of non-linear boundary integral equation associated with a single-layer potential approach to solve the forward scattering problem. We present the mathematical foundations of the method and exhibit its feasibility by numerical examples.

1 Introduction

The problem is to determine simultaneously both the shape of the obstacle and the impedance function defined on the coated boundary from scattering of time-harmonic E-polarized electromagnetic plane waves. In the current paper we deal with dielectric scatterers covered by a thin boundary layer described by a impedance boundary condition and confine ourselves to the case of infinitely long coated homogeneous dielectric cylinders. This restriction provides us to reduce the problem into two dimension.

Let the simply connected bounded domain $D \subset \mathbb{R}^2$ with C^2 boundary Γ represent the cross section of an infinitely long coated homogeneous dielectric cylinder having constant wave number k_d with $Im\{k_d\}$, $\mathrm{Re}\{k_d\} \geqslant 0$ and denote the exterior wave number of background by $k_0 \in \mathbb{R}$. Denote by ν the outward unit normal vector to Γ. Then, given an incident plane wave $v^i = e^{ik_0 x.d}$ with incident direction given by the unit vector d, the direct scattering problem for E-polarized electromagnetic

A. Altundag (✉)
Istanbul Sabahattin Zaim University, Istanbul, Turkey
e-mail: ahmet.altundag@izu.edu.tr

G.A. Anastassiou and O. Duman (eds.), *Intelligent Mathematics II: Applied Mathematics and Approximation Theory*, Advances in Intelligent Systems and Computing 441, DOI 10.1007/978-3-319-30322-2_4

waves by a coated homogeneous dielectric is modelled by the following conductive-transmission boundary value problem for the Helmholtz equation: Find solutions $v \in H^1_{\text{loc}}(\mathbb{R}^2 \backslash \bar{D})$ and $v \in H^1(D)$ to the Helmholtz equations

$$\Delta v + k_0^2 v = 0 \quad \text{in } R^2 \backslash \bar{D}, \qquad \Delta w + k_d^2 w = 0 \quad \text{in } D \tag{1}$$

with the conductive-transmission boundary conditions

$$v = w, \qquad \frac{\partial v}{\partial \nu} = \frac{\partial w}{\partial \nu} + i\eta w \quad \text{on} \quad \Gamma \tag{2}$$

for some continuous function defined in one continuously differentiable real valued function space $\eta \in C^1(\Gamma)$ with $\eta \leq 0$ and where the total field is given by $v = v^i + v^s$ with the scattered wave v^s fulfilling the Sommerfeld radiation condition

$$\lim_{r \to \infty} r^{1/2} \left(\frac{\partial v^s}{\partial r} - i k_0 v^s \right) = 0, \quad r = |x|, \tag{3}$$

uniformly with respect to all directions. The latter is equivalent to an asymptotic behavior of the form

$$v^s(x) = \frac{e^{ik_0|x|}}{\sqrt{|x|}} \left\{ v_\infty \left(\frac{x}{|x|} \right) + O\left(\frac{1}{|x|} \right) \right\}, \quad |x| \to \infty, \tag{4}$$

uniformly in all directions, with the far field pattern v_∞ defined on the unit circle Ω in $\mathbb{R}^2$ (see [4]). In the above, v and w represent the electric field that is parallel to the cylinder axis, (1) corresponds to the time-harmonic Maxwell equations and the impedance-transmission conditions (2) model the continuity of the tangential components of the electric and magnetic field across the interface Γ.

The inverse obstacle problem we are interested in is, given the far field pattern v_∞ for one incident plane wave with incident direction $d \in \Omega$ to determine simultaneously both the boundary Γ of the scattering dielectric D and the impedance function η. More generally, we also consider the simultaneous reconstruction of Γ and η from the far field patterns for a small finite number of incident plane waves with different incident directions. This inverse problem is non-linear and ill-posed, since the solution of the scattering problem (1)–(3) is non-linear with respect to the boundary and impedance function, and since the mapping from the boundary and impedance function into the far field pattern is extremely smoothing.

For a stable solution of the inverse problem we propose an algorithm that combines the approaches suggested and investigated by Kress and Rundell [2, 3] and by Ivanyshyn and Kress [1], and extend the approaches to the case of an infinitely long coated homogeneous dielectric cylinder with arbitrarily shaped cross section embedded in a homogeneous background. Representing the solution w and v^s to the forward scattering problem in terms of single-layer potentials in D and in $\mathbb{R}^2 \backslash \bar{D}$ with densities ξ_d and ξ_0, respectively, the impedance-transmission boundary condition (2)

provides a system of two boundary integral equations on Γ for the corresponding densities, that in the sequel we will denote as field equations. For the inverse problem, the required coincidence of the far field of the single-layer potential representing v^s and the given far field v_∞ provides a further equation that we denote as data equation. The system of the field and data equations can be viewed as three equations for four unknowns, i.e., the two densities, boundary of the scatterer Γ, and the conductive function η. They are linear with respect to the densities and non-linear with respect to the impedance function and the boundary.

In the spirit of [1–3], given approximations Γ_{approx}, η_{approx}, $\xi_{d_{approx}}$, and $\xi_{0_{approx}}$ for the boundary Γ, the impedance function η, the densities ξ_d and ξ_0 we linearise simultaneously both the field and the data equation with respect to all unknowns, i.e., the boundary curve, the impedance function, and the two densities. The linear equations are then solved to update the boundary curve, the impedance function, and the two densities. Because of the ill-posedness the solution of the update equations require stabilization, for example, by Tikhonov regularization. This procedure is then iterated until some suitable stopping criterion is satisfied.

At this point we note that uniqueness results for this inverse impedance—transmission problem are only available for the case of infinitely many incident waves (see [5]). A general uniqueness result based on the far field pattern for one or finitely many incident waves is still lacking.

To some extend, the inverse problem consists in solving a certain Cauchy problem, i.e., extending a solution to the Helmholtz equation from knowing their Cauchy data on some boundary curve. With this respect we also mention the related work of Ben Hassen et al. [6], Cakoni and Colton [7], Cakoni et al. [8], Eckel and Kress [9], Fang and Zeng [10], Ivanyshyn and Kress [11], Jakubik and Potthast [12]. For the simultaneous reconstruction of the shape and the impedance function for an impenetrable scatterers in a homogeneous background we refer to Kress and Rundell [2], Liu et al. [13, 14]. For the shape or the impedance reconstruction for penetrable scatterers, i.e., for dielectric obstacles we refer to Altundag and Kress [15, 16], Altundag [17–20], Akduman et al. [21], and Yaman [22].

The plan of the paper is as follows: In Sect. 2, as ingredient of our inverse algorithm we demonstrate the solution of the forward scattering problem via a single-layer approach followed by a corresponding numerical solution method in Sect. 3. In Sect. 4, we describe our inverse algorithm via simultaneous linearisation of the field and data equation in detail. In Sect. 5, we illustrate the feasibility of the method by some numerical examples.

2 The Direct Problem

The forward scattering problem (1)–(3) has at most one solution (see Gerlach and Kress [5]). Existence can be proven via boundary integral equations by a combined single- and double-layer approach (see Gerlach and Kress [5]).

Here, as one of the ingredients of our inverse algorithm, we follow [15] and suggest a single-layer approach. For this we denote by

$$\Phi_k(x, y) := \frac{i}{4} H_0^{(1)}(k|x - y|), \quad x \neq y,$$

the fundamental solution to the Helmholtz equation with wave number k in $\mathbb{R}^2$ in terms of the Hankel function $H_0^{(1)}$ of order zero and of the first kind. Adopting the notation of [4], in a Sobolev space setting, for $k = k_d$ and $k = k_0$, we introduce the single-layer potential operators

$$S_k : H^{-1/2}(\Gamma) \to H^{1/2}(\Gamma)$$

by

$$(S_k\xi)(x) := 2 \int_\Gamma \Phi_k(x, y)\xi(y)\, ds(y), \quad x \in \Gamma, \tag{5}$$

and the normal derivative operators

$$K_k' : H^{-1/2}(\Gamma) \to H^{-1/2}(\Gamma)$$

by

$$(K_k'\xi)(x) := 2 \int_\Gamma \frac{\partial \Phi_k(x, y)}{\partial \nu(x)} \xi(y)\, ds(y), \quad x \in \Gamma. \tag{6}$$

For the Sobolev spaces and the mapping properties of these operators we refer to [23, 24].

Then, from the jump relations it can be seen that the single-layer potentials

$$\begin{aligned} w(x) &= \int_\Gamma \Phi_{k_d}(x, y)\xi_d(y)\, ds(y), \quad x \in D, \\ v^s(x) &= \int_\Gamma \Phi_{k_0}(x, y)\xi_0(y)\, ds(y), \quad x \in \mathbb{R}^2 \backslash \bar{D}, \end{aligned} \tag{7}$$

solve the scattering problem (1)–(3) provided the densities ξ_d and ξ_0 fulfil the system of integral equations

$$\begin{aligned} S_{k_d}\xi_d - S_{k_0}\xi_0 &= 2v^i|_\Gamma, \\ \xi_d + \xi_0 + i\eta S_{k_d}\xi_d + K_{k_d}'\xi_d - K_{k_0}'\xi_0 &= 2 \left. \frac{\partial v^i}{\partial \nu} \right|_\Gamma. \end{aligned} \tag{8}$$

Provided k_0 is not a Dirichlet eigenvalue of the negative Laplacian for D, (7) has at most one solution. For the existence analysis and uniqueness of a solution, we refer to [19].

3 Numerical Solution

For the numerical solution of (8) and the presentation of our inverse algorithm we assume that the boundary curve Γ is given by a regular 2π-periodic parameterization

$$\Gamma = \{\zeta(s) : 0 \le s \le 2\pi\}. \tag{9}$$

Then, via $\chi = \xi \circ \zeta$. emphasizing the dependence of the operators on the boundary curve, we introduce the parameterized single-layer operator

$$\widetilde{S}_k : H^{-1/2}[0, 2\pi] \times C^2[0, 2\pi] \to H^{1/2}[0, 2\pi]$$

by

$$\widetilde{S}_k(\chi, \zeta)(s) := \frac{i}{2} \int_0^{2\pi} H_0^{(1)}(k|\zeta(s) - \zeta(\tau)|)\, |\zeta'(\tau)|\, \chi(\tau)\, d\tau$$

and the parameterized normal derivative operators

$$\widetilde{K}'_k : H^{-1/2}[0, 2\pi] \times C^2[0, 2\pi] \to H^{-1/2}[0, 2\pi]$$

by

$$\begin{aligned}\widetilde{K}'_k(\chi, \zeta)(s) := \frac{ik}{2} \int_0^{2\pi} & \frac{[\zeta'(s)]^\perp \cdot [\zeta(\tau) - \zeta(s)]}{|\zeta'(s)|\, |\zeta(s) - \zeta(\tau)|} \\ & \times H_1^{(1)}(k|\zeta(s) - \zeta(\tau)|)\, |\zeta'(\tau)|\, \chi(\tau)\, d\tau\end{aligned}$$

for $s \in [0, 2\pi]$. Here we made use of $H_0^{(1)\prime} = -H_1^{(1)}$ with the Hankel function $H_1^{(1)}$ of order zero and of the first kind. Furthermore, we write $\zeta^\perp = (\zeta_2, -\zeta_1)$ for a vector $\zeta = (\zeta_1, \zeta_2)$, that is, $\zeta^\perp$ is obtained by rotating ζ clockwise by 90°. Then the parameterized form of (8) is given by

$$\begin{aligned}\widetilde{S}_{k_d}(\chi_d, \zeta) - \widetilde{S}_{k_0}(\chi_0, \zeta) &= 2\, v^i \circ \zeta, \\ \chi_d + \chi_0 + (\eta \circ \zeta)\widetilde{S}_{k_d}(\chi_d, \zeta) & \\ + \widetilde{K}'_{k_d}(\chi_d, \zeta) - \widetilde{K}'_{k_0}(\chi_0, \zeta) &= \frac{2}{|\zeta'|}\, [\zeta']^\perp \cdot \operatorname{grad} v^i \circ \zeta.\end{aligned} \tag{10}$$

The kernels

$$A(s,\tau) := \frac{i}{2}\, H_0^{(1)}(k|\zeta(t)-\zeta(\tau)|)\,|\zeta'(\tau)|$$

and

$$B(s,\tau) := \frac{ik}{2}\,\frac{[\zeta'(s)]^{\perp}\cdot[\zeta(\tau)-\zeta(s)]}{|\zeta'(s)|\,|\zeta(s)-\zeta(\tau)|}\, H_1^{(1)}(k|\zeta(s)-\zeta(\tau)|)\,|\zeta'(\tau)|$$

of the operators $\widetilde{S}_k$ and $\widetilde{K}'_k$ can be written in the form

$$\begin{aligned} A(s,\tau) &= A_1(s,\tau)\ln\left(4\sin^2\tfrac{s-\tau}{2}\right) + A_2(s,\tau),\\ B(s,\tau) &= B_1(s,\tau)\ln\left(4\sin^2\tfrac{s-\tau}{2}\right) + B_2(s,\tau), \end{aligned} \tag{11}$$

where

$$A_1(s,\tau) := -\frac{1}{2\pi}\, J_0(k|\zeta(s)-\zeta(\tau)|)|\zeta'(\tau)|,$$

$$A_2(s,\tau) := A(s,\tau) - A_1(s,\tau)\ln\left(4\sin^2\frac{s-\tau}{2}\right),$$

$$B_1(s,\tau) := -\frac{k}{2\pi}\,\frac{[\zeta'(s)]^{\perp}\cdot[\zeta(\tau)-\zeta(s)]}{|\zeta'(s)|\,|\zeta(s)-\zeta(\tau)|}\, J_1(k|\zeta(s)-\zeta(\tau)|)\,|\zeta'(\tau)|,$$

$$B_2(s,\tau) := B(s,\tau) - B_1(s,\tau)\ln\left(4\sin^2\frac{s-\tau}{2}\right).$$

J_0 and J_1 denote the Bessel functions of order zero and one respectively. The functions A_1, A_2, B_1, and B_2 turn out to be analytic with diagonal terms

$$A_2(s,s) = \left[\frac{i}{2} - \frac{C}{\pi} - \frac{1}{\pi}\ln\left(\frac{k}{2}|\zeta'(s)|\right)\right]|\zeta'(s)|$$

in terms of Euler's constant C and

$$B_2(s,s) = -\frac{1}{2\pi}\,\frac{[\zeta'(s)]^{\perp}\cdot\zeta''(s)}{|\zeta'(s)|^2}\,.$$

For integral equations with kernels of the form (11) a combined collocation and quadrature methods based on trigonometric interpolation as described in Sect. 3.5 of [4] or in [25] is at our disposal. We refrain from repeating the details. For a related

error analysis we refer to [23] and note that we have exponential convergence for smooth, i.e., analytic boundary curves Γ.

For a numerical example, we consider the scattering of a plane wave by a dielectric cylinder with a non-convex apple-shaped cross section with boundary Γ described by the parametric representation

$$\zeta(s) = \left\{ \frac{0.5 + 0.4\cos s + 0.1\sin 2s}{1 + 0.7\cos s}(\cos s, \sin s) : s \in [0, 2\pi] \right\} \tag{12}$$

The following impedance functions are chosen in our experiments.

- $$\eta_1 = -1 - 0.5\sin(s) \tag{13}$$

- $$\eta_2 = -2 - \cos(2s) - 0.5\sin(s) \tag{14}$$

From the asymptotics for the Hankel functions, it can be deduced that the far field pattern of the single-layer potential v^s with density ξ_0 is given by

$$v_\infty(\hat{x}) = \gamma \int_\Gamma e^{-ik_0 \hat{x}\cdot y} \xi_0(y)\, ds(y), \quad \hat{x} \in \Omega, \tag{15}$$

where

$$\gamma = \frac{e^{i\frac{\pi}{4}}}{\sqrt{8\pi k_0}}.$$

The latter expression can be evaluated by the composite trapezoidal rule after solving the system of integral equations (8) for ξ_0, i.e., after solving (10) for χ_0. Table 1 gives some approximate values for the far field pattern $v_\infty(d)$ and $v_\infty(-d)$ in the forward direction d and the backward direction $-d$. The direction d of the incident wave is $d = (1, 0)$ and the wave numbers are $k_0 = 1$ and $k_d = 4 + 1i$, and the conductive function η_2 in (14) is chosen. Note that the exponential convergence is clearly exhibited.

Table 1 Numerical results for direct scattering problem

n	$\mathrm{Re}\, u_\infty(d)$	$\mathrm{Im}\, u_\infty(d)$	$\mathrm{Re}\, u_\infty(-d)$	$\mathrm{Im}\, u_\infty(-d)$
8	−0.9246701916	0.1927903437	−0.9330234793	0.2054859030
16	−0.9246830723	0.1927431421	−0.9330023078	0.2053750332
32	−0.9246871867	0.1927361525	−0.9330054172	0.2053781827
64	−0.9246871412	0.1927360822	−0.9330054392	0.2053782645

4 The Inverse Problem

We now proceed describing an iterative algorithm for approximately solving the inverse scattering problem by combining the method proposed by Ivanyshyn, Kress and Rundell [1–3] and by extending from the case of impenetrable obstacles to the case of penetrable scatterers. After introducing the far field operator $S_\infty : H^{-1/2}(\Gamma) \to L^2(\Omega)$ by

$$(S_\infty \varphi)(\hat{x}) := \gamma \int_\Gamma e^{-ik_0 \hat{x}\cdot y} \xi(y)\, ds(y), \quad \hat{x} \in \Omega, \tag{16}$$

from (7) and (15) we observe that the far field pattern for the solution to the scattering problem (1)–(3) is given by

$$v_\infty = S_\infty \xi_0 \tag{17}$$

in terms of the solution to (8). Thus as theoretical basis of our inverse algorithm we can state the following theorem.

Theorem 1 *For a given incident field v^i and a given far field pattern v_∞, assume that the boundary Γ, the impedance function η, and the densities ξ_d and ξ_0 satisfy the system of three integral equations*

$$\begin{aligned} S_{k_d}\xi_d - S_{k_0}\xi_0 &= 2v^i, \\ \xi_d + \xi_0 + i\eta S_{k_d}\xi_d + K'_{k_d}\xi_d - K'_{k_0}\xi_0 &= 2\frac{\partial v^i}{\partial \nu}, \\ S_\infty \xi_0 &= v_\infty. \end{aligned} \tag{18}$$

Then Γ and η solve the inverse scattering problem.

The ill-posedness of the inverse problem is reflected through the ill-posedness of the third integral equation, the far field equation that we denote as *data equation.* Note that (18) is linear with respect to the densities and nonlinear with respect to the boundary Γ and the impedance function η. This opens up a variety of approaches to solve (18) by linearization and iteration. In the current paper, we are going to proceed as follows: Given approximations Γ_{approx} and η_{approx} for the boundary Γ and the impedance function η, and approximations $\xi_{d_{approx}}$ and $\xi_{0_{approx}}$ for the densities ξ_d and ξ_0 we linearise simultaneously both the field and the data equations with respect to the boundary curve, the impedance function and the two densities. The linear equations are then solved to update the boundary curve, the conductive function and the two densities. Because of the ill-posedness the solution of the update equations require stabilization. For this, we use Tikhonov regularization. This procedure is then iterated until some suitable stopping criterion is achieved.

To describe this in more detail, we also require the parameterized version

$$\widetilde{S}_\infty : H^{-1/2}[0, 2\pi] \times C^2[0, 2\pi] \to L^2(\Omega)$$

of the far field operator as given by

$$\widetilde{S}_\infty(\chi, \zeta)(\hat{x}) := \gamma \int_0^{2\pi} e^{-ik_0 \hat{x}\cdot\zeta(\tau)} |\zeta'(\tau)| \chi(\tau)\, d\tau, \quad \hat{x} \in \Omega. \tag{19}$$

Then the parameterized form of (18) is given by

$$\begin{aligned} \widetilde{S}_{k_d}(\chi_d, \zeta) - \widetilde{S}_{k_0}(\chi_0, \zeta) &= 2\, v^i \circ \zeta, \\ \chi_d + \chi_0 + i(\eta \circ \zeta)\widetilde{S}_{k_d}(\chi_d, \zeta) & \\ + \widetilde{K}'_{k_d}(\chi_d, \zeta) - \widetilde{K}'_{k_0}(\chi_0, \zeta) &= \frac{2}{|\zeta'|}\, [\zeta']^\perp \cdot \operatorname{grad} v^i \circ \zeta, \\ \widetilde{S}_\infty(\chi_0, z) &= v_\infty. \end{aligned} \tag{20}$$

For a fixed χ the Fréchet derivative of the operator $\widetilde{S}_k$ and $\widetilde{K}'_k$ with respect to the boundary ζ in the direction h are given by

$$\begin{aligned} \partial \widetilde{S}_k(\chi, \zeta; h)(s) = \frac{-ik}{2} \int_0^{2\pi} & \frac{(\zeta(s) - \zeta(\tau)) \cdot (h(s) - h(\tau))}{|\zeta(s) - \zeta(\tau)|} \\ & \times |\zeta'(\tau)|\, H_1^{(1)}(k|\zeta(s) - \zeta(\tau)|)\chi(\tau) d\tau \\ & + \frac{i}{2} \int_0^{2\pi} \frac{\zeta'(\tau) \cdot h'(\tau)}{|\zeta'(\tau)|} H_0^{(1)}(k|\zeta(t) - \zeta(\tau)|)\chi(\tau) d\tau, \end{aligned}$$

and

$$\begin{aligned} & \partial \widetilde{K}'_k(\chi, \zeta; h)(s) \\ & = -\frac{ik}{2|\zeta'(s)|} \int_0^{2\pi} \frac{[\zeta'^{\perp}\cdot(h(s) - h(\tau)) + [h'^{\perp}\cdot(\zeta(s) - \zeta(\tau))}{|\zeta(s) - \zeta(\tau)|} \\ & \times |\zeta'(\tau)| H_1^{(1)}(k|\zeta(s) - \zeta(\tau)|)\chi(\tau) d\tau \\ & + \frac{ik}{|\zeta'(s)|} \int_0^{2\pi} \frac{[\zeta'^{\perp}\cdot(\zeta(s) - \zeta(\tau))(h(s) - h(\tau)) \cdot (\zeta(s) - \zeta(\tau))}{|\zeta(s) - \zeta(\tau)|^3} \\ & \times |\zeta'(\tau)| H_1^{(1)}(k|\zeta(s) - \zeta(\tau)|)\chi(\tau) d\tau \end{aligned} \tag{21}$$

$$
\begin{aligned}
&-\frac{ik^2}{2|\zeta'(s)|}\int_0^{2\pi}\frac{[\zeta'^{\perp}\cdot(\zeta(s)-\zeta(\tau))(h(s)-h(\tau))\cdot(\zeta(s)-\zeta(\tau))}{|\zeta(s)-\zeta(\tau)|^2}\\
&\times|\zeta'(\tau)|H_0^{(1)}(k|\zeta(s)-\zeta(\tau)|)\chi(\tau)d\tau\\
&+\frac{ik}{2}\frac{h'(s)\cdot\zeta'(s)}{|\zeta'^2}\int_0^{2\pi}\frac{[\zeta'^{\perp}\cdot(\zeta(s)-\zeta(\tau))}{|\zeta(s)-\zeta(\tau)|}\\
&\times|\zeta'(\tau)|H_1^{(1)}(k|\zeta(s)-\zeta(\tau)|)\chi(\tau)d\tau\\
&-\frac{ik}{2|\zeta'(s)|}\int_0^{2\pi}\frac{[\zeta'^{\perp}\cdot(\zeta(s)-\zeta(\tau))h'(\tau)\cdot\zeta'(\tau)}{|\zeta(s)-\zeta(\tau)||\zeta'(\tau)|}\\
&\times H_1^{(1)}(k|\zeta(s)-\zeta(\tau)|)\chi(\tau)d\tau.
\end{aligned}
$$

Then the linearisation (20) with respect to all variables ζ, η, χ_d and χ_0 in the direction h, θ, μ_d and μ_0, respectively, reads

$$
\begin{aligned}
&\widetilde{S}_{k_d}(\chi_d,\zeta)+\widetilde{S}_{k_d}(\mu_d,\zeta)+\partial\widetilde{S}_{k_d}(\chi_d,\zeta;h)-\widetilde{S}_{k_0}(\chi_0,\zeta)-\widetilde{S}_{k_0}(\mu_0,\zeta)\\
&\quad-\partial\widetilde{S}_{k_0}(\chi_0,\zeta;h)=2v^i\circ\zeta+2\mathrm{grad}v^i\circ\zeta\cdot h,\\
&\chi_d+\mu_d+\chi_0+\mu_0+\mathrm{i}(\theta\circ\zeta)\widetilde{S}_{k_d}(\chi_d,\zeta)+\mathrm{i}(\eta\circ\zeta)\widetilde{S}_{k_d}(\chi_d,\zeta)\\
&\quad+\widetilde{K}'_{k_d}(\chi_d,\zeta)+\widetilde{K}'_{k_d}(\mu_d,\zeta)+\partial\widetilde{K}'_d(\chi_d,\zeta;h)\\
&-\widetilde{K}'_{k_0}(\chi_0,\zeta)-\widetilde{K}'_{k_0}(\mu_0,\zeta)-\partial\widetilde{K}'_{k_0}(\chi_0,\zeta;h)\\
&\quad=\frac{2}{|\zeta'|}[\zeta'^{\perp}\cdot\mathrm{grad}v^i\circ\zeta+2\sigma(\zeta)\cdot h,\\
&\widetilde{S}_{\infty}(\chi_0,\zeta)+\widetilde{S}_{\infty}(\mu_0,\zeta)+\partial\widetilde{S}_{\infty}(\chi_0,\zeta;h)=v_{\infty}.
\end{aligned}
\tag{22}
$$

Here the term $\sigma(\zeta)\cdot h$ is the form (see [26])

$$
\sigma(\zeta)\cdot h=-\frac{\partial v^i}{\partial\tau}\frac{\nu\cdot h'}{|\zeta'|}+(\frac{\partial^2 v^i}{\partial\nu\partial\tau}-H\frac{\partial v^i}{\partial\tau})\tau\cdot h+\frac{\partial^2 v^i}{\partial\nu^2}\nu\cdot h \tag{23}
$$

and τ and H stand for the tangential vector and the mean curvature respectively. They are given by

$$
\tau=\frac{\zeta'}{|\zeta'|},\quad\text{and}\quad H=-\frac{\zeta''\cdot\nu}{|\zeta'^2}
$$

and the matrix form of (22) can be written as

$$\begin{bmatrix} \{\partial \widetilde{S}_{k_d}(\chi_d,\zeta;.) - \partial \widetilde{S}_{k_0}(\chi_0,\zeta;.) \\ -2\mathrm{grad}v^i \circ \zeta; Zeros\} & \widetilde{S}_{k_d}(.,\zeta) & -\widetilde{S}_{k_d}(.,\zeta) \\ \{\partial \widetilde{K}'_{k_d}(\chi_d,\zeta;.) - \partial \widetilde{K}'_{k_0}(\chi_0,\zeta;.) \\ -\xi(\zeta); \mathrm{i}\widetilde{S}_{k_d}\chi_d\} & I + \widetilde{K}'_{k_d}(.,\zeta) & I - \widetilde{K}'_{k_d}(.,\zeta) \\ \partial \widetilde{S}_\infty(\chi_0,\zeta;.); Zeros & 0 & \widetilde{S}_\infty(.,\zeta) \end{bmatrix} \begin{bmatrix} [h;\theta] \\ \mu_d \\ \mu_0 \end{bmatrix}$$

$$= \begin{bmatrix} 2v^i \circ \zeta - \widetilde{S}_{k_d}(\chi_d,\zeta) + \widetilde{S}_{k_0}(\chi_0,\zeta) \\ \left\{ \frac{2}{|\zeta'|}[\zeta'^{\perp} \cdot \mathrm{grad}\mathrm{v}^{\mathrm{i}} \circ \zeta - \chi_{\mathrm{d}} - \widetilde{\mathrm{K}}'_{\mathrm{k_d}}(\chi_{\mathrm{d}},\zeta) - \chi_0 \right. \\ \left. + \widetilde{\mathrm{K}}'_{\mathrm{k_0}}(\chi_0,\zeta) - \mathrm{i}(\eta \circ \zeta)\widetilde{\mathrm{S}}_{\mathrm{k_d}}(\chi_{\mathrm{d}},\zeta)\right\} \\ v_\infty - \widetilde{S}_\infty(\chi_0,\zeta) \end{bmatrix} \tag{24}$$

Now we can describe the method in a short form as follows:
Each iteration step of the proposed inverse algorithm consists of one part.

- Given an approximation ζ for the boundary, η for the conductive function, and χ_d, χ_0 for the densities, we solve the linearized sistem of integral equation (24), for h, θ, μ_d, and μ_0 to obtain updates $\zeta + h$, $\eta + \theta$, $\chi_d + \mu_d$, and $\chi_0 + \mu_0$. We continue this procedure until some stopping criteria is achieved. The stopping criterion for the iterative scheme is given by the relative error

$$\frac{\| v_{\infty;N} - v_\infty \|}{\| v_\infty \|} \leq \epsilon(\delta),$$

where $v_{\infty;N}$ is the computed far field pattern after N iteration steps.

As a theoretical basis for the application of Tikhonov regularization from [27] we cite that, after the restriction to star-like boundaries, the operator $\partial \widetilde{S}_\infty$ is injective provided k_0^2 is not a Neumann eigenvalue for the negative Laplacian in D.

5 Numerical Examples

To avoid an inverse crime, in our numerical examples the synthetic far field data were obtained by a numerical solution of the boundary integral equations based on a combined single- and double-layer approach (see [28, 29]) using the numerical schemes as described in [4, 23, 30]. In each iteration step of the inverse algorithm for the solution of the matrix equation (24) we used the numerical method described in Sect. 3 using 64 quadrature points. The linearized matrix equation (24) were solved

Table 2 Boundary curves

Types	Representations
Apple-shaped	$\zeta(s) = \{\frac{0.5+0.4\cos s+0.1\sin 2s}{1+0.7\cos s}(\cos s, \sin s) : s \in [0, 2\pi]\}$
Kite-shaped	$\zeta(s) = \{(\cos s + 1.3\cos^2 s - 1.3, 1.5\sin s) : s \in [0, 2\pi]\}$
Peanut-shaped	$\zeta(s) = \{\sqrt{\cos^2 s + 0.25\sin s}\,(\cos s, \sin s) : s \in [0, 2\pi]\}$
Rounded triangle	$\zeta(s) = \{(2 + 0.3\cos 3s)(\cos s, \sin s) : s \in [0, 2\pi]\}$

by Tikhonov regularization with an H^2 penalty term, i.e., $p = 2$. The regularized equation is solved by Nyström's method with the composite trapezoidal rule again using 64 quadrature points.

In all our four examples we used an incident wave with the direction $d = (1, 0)$ and $J = 5$ as degree for the approximating trigonometric polynomials for the boundary curve, $P = 3$ as degree for the approximating trigonometric polynomials for the conductive function, $\alpha = 10^{-6}$ as regularization parameter for the data equation, and the wave numbers $k_0 = 1$ and $k_d = 5 + 1\mathrm{i}$.

For simplicity, for the stopping rule we chose $\epsilon(\delta)$ the same for all noise levels since this already gave satisfactory reconstructions.

In according with the general convergence results on regularized Gauss–Newton method (see [31]) for the regularization parameters we used decreasing sequences

$$\lambda_{1,n} = \tau_1^{-n}\lambda_1$$
$$\lambda_{2,n} = \tau_2^{-n}\lambda_2$$

with $\lambda_1,\ \lambda_2$ positive and $\tau_1,\ \tau_2 > 1$ chosen by trial and error. The iteration numbers and the regularization parameters λ_1 and λ_2 for the Tikhonov regularization of boundary ζ and conductive function η, respectively, were chosen by trial and error and their values are indicated in the following description of the individual examples.

In order to obtain noisy data, random errors are added point-wise to v_∞,

$$\widetilde{v}_\infty = v_\infty + \delta\rho\frac{||v_\infty||}{|\rho|}$$

with the random variable $\rho \in \mathbb{C}$ and $\{\mathrm{Re}\rho, \mathrm{Im}\rho\} \in (0, 1)$. For all examples, 2 % noise level, i.e., $\delta = 0.02$ is added into the far-field pattern.

In the first example Fig. 1 illustrates reconstructions after 10 iterations with the regularization parameters $\lambda_1 = 0.7,\ \tau_1 = 1.1$ and $\lambda_2 = 1.2,\ \tau_2 = 1.15$.

In the second example Fig. 2 shows reconstructions after 15 iterations with the regularization parameter chosen as in the first example.

In the third example the reconstructions in Fig. 3 were obtained after 13 iterations with the regularization parameter chosen as in the first example.

In the fourth example the reconstructions in Fig. 4 were obtained after 15 iterations with the regularization parameters chosen as $\lambda_1 = 1.3,\ \tau_1 = 1.1$ and $\lambda_2 = 0.8,\ \tau_2 = 1.5$.

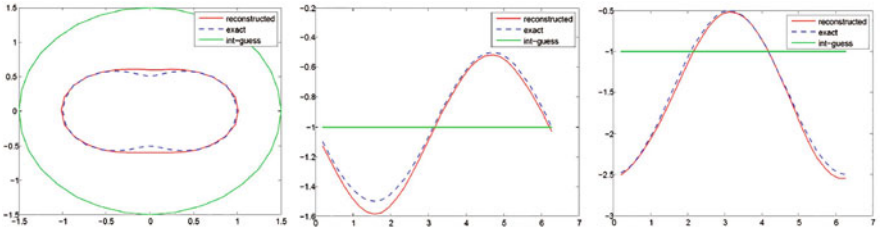

Fig. 1 Reconstruction of the peanut-shaped contour in Table 2 (*left*), conductive function η_1 in (13) (*middle*), and η_2 in (14) (*right*)

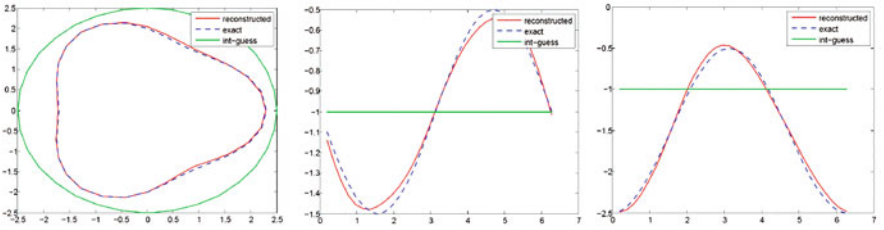

Fig. 2 Reconstruction of the rounded-shaped contour in Table 2 (*left*), conductive function η_1 in (13) (*middle*), and η_2 in (14) (*right*)

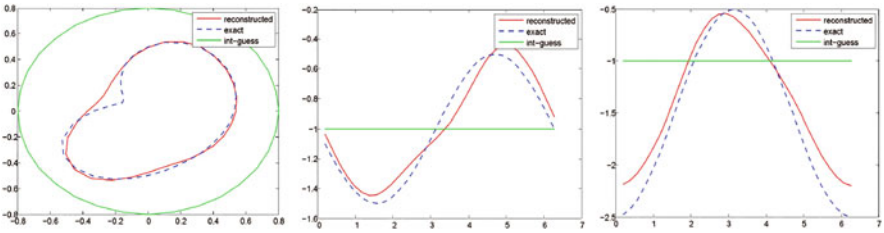

Fig. 3 Reconstruction of the apple-shaped contour in Table 2 (*left*), conductive function η_1 in (13) (*middle*), and η_2 in (14) (*right*)

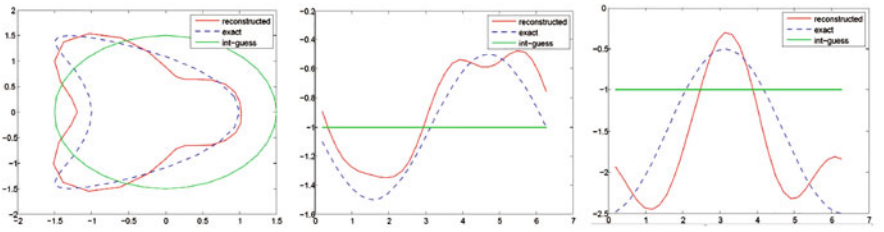

Fig. 4 Reconstruction of the kite-shaped contour in Table 2 (*left*), conductive function η_1 in (13) (*middle*), and η_2 in (14) (*right*)

Our examples clearly indicate the feasibility of the proposed algorithm with a reasonable stability against noise. An appropriate initial guess was important to ensure numerical convergence of the iterations. Further research will be directed towards applying the algorithm to real data, to extend the numerics to the three dimensional case.

Acknowledgments The author would like to thank Professor Rainer Kress for the helpful discussions and suggestions on the topic of this paper.

References

1. Ivanyshyn, O., Kress, R.: Nonlinear integral equations in inverse obstacle scattering. In: Fotiatis, D., Massalas, C. (eds.) Mathematical Methods in Scattering Theory and Biomedical Engineering. World Scientific, Singapore, pp. 39–50 (2006)
2. Kress, R., Rundell, W.: Inverse scattering problem for shape and impedance. Inverse Prob. **17**, 1075–1085 (2001)
3. Kress, R., Rundell, W.: Nonlinear integral equations and the iterative solution for an inverse boundary value problem. Inverse Prob. **21**, 1207–1223 (2005)
4. Colton, D., Kress, R.: Inverse Acoustic and Electromagnetic Scattering Theory, 2nd edn. Springer, Berlin (1998)
5. Gerlach, T., Kress, R.: Uniqueness in inverse obstacle scattering with conductive boundary condition. Inverse Prob. **12**, 619–625 (1996)
6. Hassen, M.F.B., Ivanyshyn, O., Sini, M.: The 3D acoustic scattering by complex obstacles. Inverse Prob. **26**, 105–118 (2010)
7. Cakoni, F., Colton, D.: The determination of the surface impedance of a partially coated obstacle from the far field data. SIAM J. Appl. Math. **64**, 709–723 (2004)
8. Cakoni, F., Colton, D., Monk, P.: The determination of boundary coefficients from far field measurements. J. Integr. Eqn. Appl. **22**, 167–191 (2010)
9. Eckel, H., Kress, R.: Nonlinear integral equations for the inverse electrical impedance problem. Inverse Prob. **23**, 475–491 (2007)
10. Fang, W., Zeng, S.: A direct solution of the Robin inverse problem. J. Integr. Eqn. Appl. **21**, 545–557 (2009)
11. Ivanyshyn, O., Kress, R.: Inverse scattering for surface impedance from phase-less far field data. J. Comput. Phys. **230**, 3443–3452 (2011)
12. Jakubik, P., Potthast, R.: Testing the integrity of some cavity-the Cauchy problem and the range test. Appl. Numer. Math. **58**, 899–914 (2008)
13. Liu, J., Nakamura, G., Sini, M.: Reconstruction of the shape and surface impedance from acoustic scattering data for arbitrary cylinder. SIAM J. Appl. Math. **67**, 1124–1146 (2007)
14. Nakamura, G., Sini, M.: Reconstruction of the shape and surface impedance from acoustic scattering data for arbitrary cylinder. SIAM J. Anal. **39**, 819–837 (2007)
15. Altundag, A., Kress, R.: On a two dimensional inverse scattering problem for a dielectric. Appl. Anal. **91**, 757–771 (2012)
16. Altundag, A., Kress, R.: An iterative method for a two-dimensional inverse scattering problem for a dielectric. J. Inverse Ill-Posed Prob. **20**, 575–590 (2012)
17. Altundag, A.: On a two-dimensional inverse scattering problem for a dielectric, Dissertation, Göttingen, Feb 2012
18. Altundag, A.: A hybrid method for inverse scattering problem for a dielectric. In: Advances in Applied Mathematics and Approximation Theory, vol. 41, pp. 185–203. Springer (2013)
19. Altundag, A.: Inverse obstacle scattering with conductive boundary condition for a coated dielectric cylinder. J. Concr. Appl. Math. **13**, 11–22 (2015)

20. Altundag, A.: A second degree Newton method for an inverse scattering problem for a dielectric. Hittite J. Sci. Eng. **2**, 115–125 (2015)
21. Akduman, I., Kress, R., Yaman, F., Yapar, A.: Inverse scattering for an impedance cylinder buried in a dielectric cylinder. Inverse Prob. Sci. Eng. **17**, 473–488 (2009)
22. Yaman, F.: Location and shape reconstructions of sound-soft obstacle buried in penetrable cylinders. Inverse Prob. **25**, 1–17 (2009)
23. Kress, R.: Integral Equation, 2nd edn. Springer, Berlin (1998)
24. McLean, W.: Strongly Elliptic Systems and Boundary Integral Equations. Cambridge University Press (2000)
25. Kress, R., Sloan, I.H.: On the numerical solution of a logarithmic integral equation of the first kind for the Helmholtz equation. Numerische Mathematik **66**, 199–214 (1993)
26. Serranho, P.: A hybrid method for inverse scattering for shape and impedance. Inverse Prob. **22**, 663–680 (2006)
27. Ivanyshyn, O., Johansson, T.: Boundary integral equations for acoustical inverse sound-soft scattering. J. Inverse Ill-Posed Prob. **15**, 1–14 (2007)
28. Colton, D., Kress, R.: Integral Equation Methods in Scattering Theory. Wiley-Interscience Publications, New York (1983)
29. Kress, R., Roach, G.F.: Transmission problems for the Helmholtz equation. J. Math. Phys. **19**, 1433–1437 (1978)
30. Kress, R.: On the numerical solution of a hypersingular integral equation in scattering theory. J. Comput. Appl. Math. **61**, 345–360 (1995)
31. Burger, M., Kaltenbacher, B., Neubauer, A.: Iterative solution methods. In: Scherzer (ed.) Handbook of Mathematical Methods in Imaging. Springer, Berlin, pp. 345–384 (2011)